Nanoscale Res Lett (2010) 5:898–903
DOI 10.1007/s11671-010-9581-6

NANO EXPRESS

Growth of In_2O_3 Nanowires Catalyzed by Cu via a Solid–Liquid–Solid Mechanism

Guanbi Chen · Lei Wang · Xia Sheng · Hongjuan Liu · Xiaodong Pi · Yuanyuan Zhang · Dongsheng Li · Deren Yang

Received: 30 December 2009 / Accepted: 16 March 2010 / Published online: 27 March 2010

Abstract In_2O_3 nanowires that are 10–50 nm in diameter and several hundred nanometers to micrometers in length have been synthesized by simply annealing Cu–In compound at a relatively low temperature of 550°C. The catalysis of Cu on the growth of In_2O_3 nanowires is investigated. It is believed that the growth of In_2O_3 nanowires is via a solid–liquid–solid (SLS) mechanism. Moreover, photoluminescence (PL) peaks of In_2O_3 nanowires at 412 and 523 nm were observed at room temperature, and their mechanism is also discussed.

Keywords In_2O_3 nanowire · SLS · Cu catalyzed · PL

Introduction

One-dimensional nanowires are one of the most important types of nanomaterials with great potential applications in nanoelectronics and photoelectronics [1, 2]. Due to the interesting optical and electrical properties, In_2O_3 with direct bandgap of around 3.6 eV has enabled many kinds of applications, such as window heaters, solar cells [1, 2], field-effect transistors [3], field emission devices [4], and various sensors [5–7]. Last decades, intense investigation of In_2O_3 nanowires has been made. Up to now, In_2O_3 nanowires have been synthesized by a variety of methods. These methods fall into two categories depending on whether a catalyst is used or not during nanowires growth. Without catalysts, In_2O_3 nanowires can be synthesized via a vapor–solid (VS) mechanism by carbonthermal evaporation [10–12], or by directly thermal evaporation of In particles [14]. Patterning by use of templates [8, 9] and oxidation of indium compound [13] have also been conducted to synthesize In_2O_3 nanowires in the absence of catalysts. When catalysts are used, nanowires can be synthesized on different substrates by a vapor–liquid–solid (VLS) mechanism [15–17]. Even vertical arrays can be grown under special conditions [18], mostly by using Au catalyst. Other catalysts such as Ag and In have also been reported [19, 20].

Although Cu has been used as the catalyst for the growth of Si and Ge nanowires due to its advantage [21, 22], the use of Cu to catalyze the growth of In_2O_3 nanowires has not been reported yet. Moreover, under common VLS conditions In vapor is needed for the growth of In_2O_3 nanowires. This means that a relatively high temperature is required to vaporize In during the growth. In this study, solid Cu–In compound was first used to successfully synthesize In_2O_3 nanowires at a relatively low temperature of 550°C. In the experiment, Cu acts as the catalyst to the nanowires, and In solid instead of In vapor works as In source so as to decrease largely the synthesizing temperature. And a solid–liquid–solid (SLS) mechanism was used to explain the growth of the nanowires.

Experimental Section

In and Cu–In compound nanoparticles were synthesized by using a polyol method. In brief, 1 mmol $InCl_3 \cdot 4H_2O$ and 0.2 g poly(vinyl pyrrolidone) (PVP, K30) were dissolved into 25 ml diethylene glycol (DEG) under N_2 at 140°C. Several drops of freshly made $NaBH_4$/tetraethylene glycol (TEG) solution (0.2 g in 5 ml TEG) were added. The

G. Chen · L. Wang (✉) · X. Sheng · H. Liu · X. Pi · Y. Zhang · D. Li · D. Yang
State Key Laboratory of Silicon Materials and Department of Materials Science and Engineering, Zhejiang University, Hangzhou 310027, People's Republic of China
e-mail: phy_wangl@dial.zju.edu.cn

particles continued to grow for 3 min. As for Cu–In nanoparticles, the same experimental procedure was used, in which 1 mmol $CuCl_2 \cdot 2H_2O$ and 1 mmol $InCl_3 \cdot 4H_2O$ were added. The products were separated by centrifugation and washed several times by ethanol. Pure In particles with diameters of 10–150 nm, and Cu–In compound particles with particle sizes of 100–500 nm were obtained, respectively. All the nanoparticles were centrifuged and washed several times with ethanol to reduce the reacting solvent. They were then dissolved in ethanol for further use. Carefully washed glass substrates were coated with the nanoparticles/ethanol solution by drop casting. The samples were subsequently transferred into a chemical vapor deposition (CVD) chamber. Annealing at 550°C was carried out for 1–2 h at a pressure of 1000 Pa in H_2/N_2 (1:9) atmosphere. After annealing, the color of Cu–In films changed from black to gray, whereas that of In films hardly changed. Additionally, for comparison, In films on Cu substrates were also prepared for the above-mentioned procedure. During the preparation of Cu substrates, they were carefully washed by ultrasonic in ethanol and rinsed with diluted hydrochloric acid.

X-ray diffraction (XRD) was carried out to study the crystal structures of all the samples by using an X'Pert PRO (PANalytical) diffractometer equipped with a Cu Kα radiation source. Data were collected by step-scanning of 2θ from 20° to 70° with a step of 0.02° and counting time of 1 s per step. Morphology of the samples was investigated by scanning electron microscopy (SEM, Hitachi S4800). Transmission electron microscopy (TEM, Philips CM200) was performed at an acceleration voltage of 160 kV. High-resolution transmission electron microscopy (HRTEM, JEM2010) was performed at an acceleration voltage of 200 kV. Differential thermal analysis (DTA) was employed to investigate the transformation process of Cu–In compound in N_2 atmosphere. Photoluminescence (PL) was collected with a Ne–Cd laser at the line of 325 nm.

Results and Discussion

Figure 1a shows an SEM image of the precursor Cu–In compound films on glass. It is clear that the metal compound is mainly composed of particles with various sizes. After annealing at 550°, nanowires that are 10–50 nm in diameter and several hundred nanometers to micrometers in length have been formed, as shown in Fig. 1b. Actually, most of them are ~20 nm in diameter, as shown in the TEM image (Fig. 1c). The winding nanowires are long and entangled. The HRTEM image in Fig. 1d demonstrates that the nanowires are monocrystalline with the lattice spacing

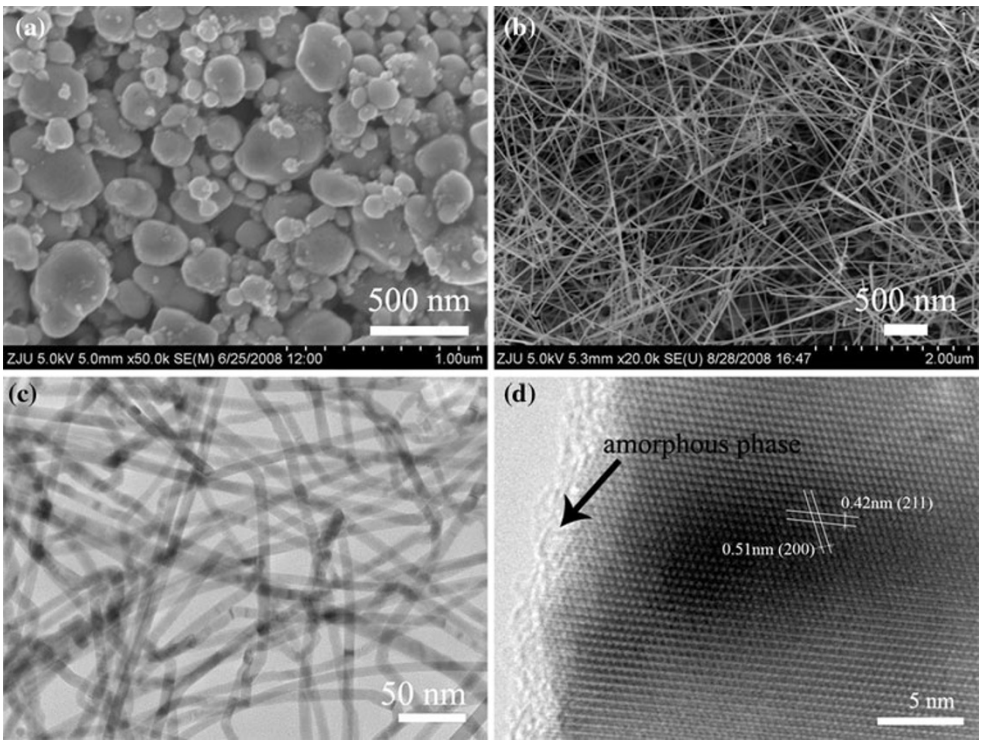

Fig. 1 **a** SEM of Cu–In compound on glass before annealing. **b** SEM, **c** TEM, and **d** HRTEM of Cu–In compound on glass after annealing for 2 h

of 0.51 and 0.42 nm, consistent with the (200) and (211) crystal plane of In_2O_3, respectively.

Figure 2 shows the XRD results for the as-grown Cu–In compound particles and annealed products. The as-grown metal compound mainly consists of In and Cu–In phases (curve A in Fig. 2). This means that the as-grown Cu–In compound is accompanied with In crystal. After annealing, it can be seen from curve B in Fig. 2 that all of the peaks are related to In_2O_3, and the three most intense peaks at 30.6°, 35.4°, and 51.0° correspond to (222), (400), and (440) planes of In_2O_3, respectively. There are no clear peaks associated with Cu–In compound or other materials. Combined with the SEM and TEM results (Fig. 1), it can be concluded that In_2O_3 nanowires are formed after annealing Cu–In compound.

To confirm the effect of Cu on the formation of In_2O_3 nanowires during annealing Cu–In compound, In particles deposited on a glass substrate or Cu substrate were also annealed at 550°C. The SEM images of the annealed

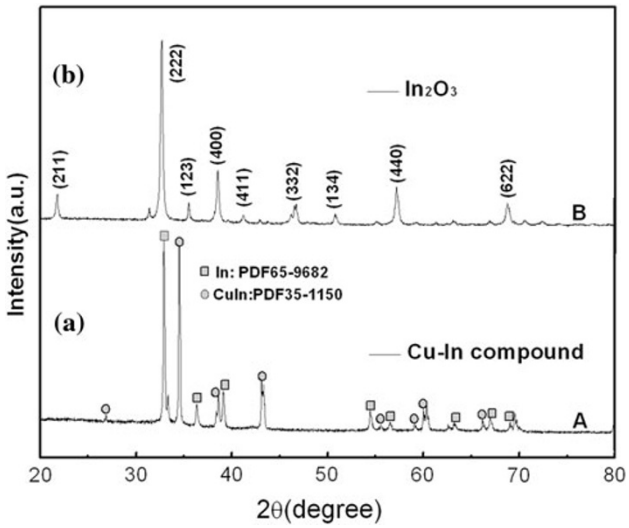

Fig. 2 XRD patterns of Cu–In compound before (curve A) and after (curve B) annealing in N_2/H_2 for 2 h on glass

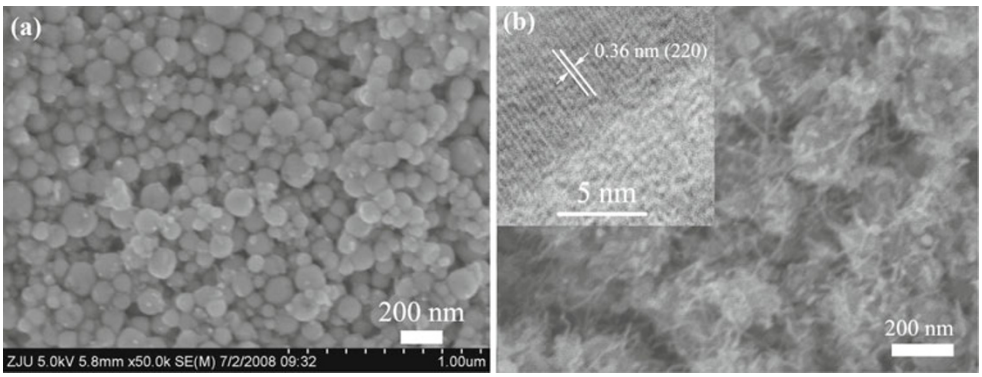

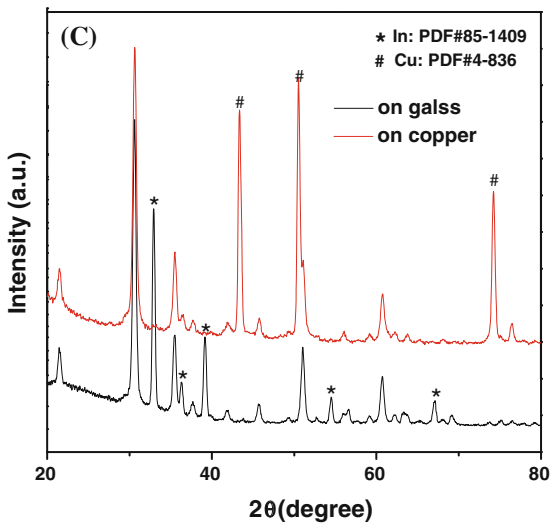

Fig. 3 SEM images of In_2O_3 nanowires synthesized by annealing In particles on **a** glass or **b** copper, and **c** corresponding XRD patterns

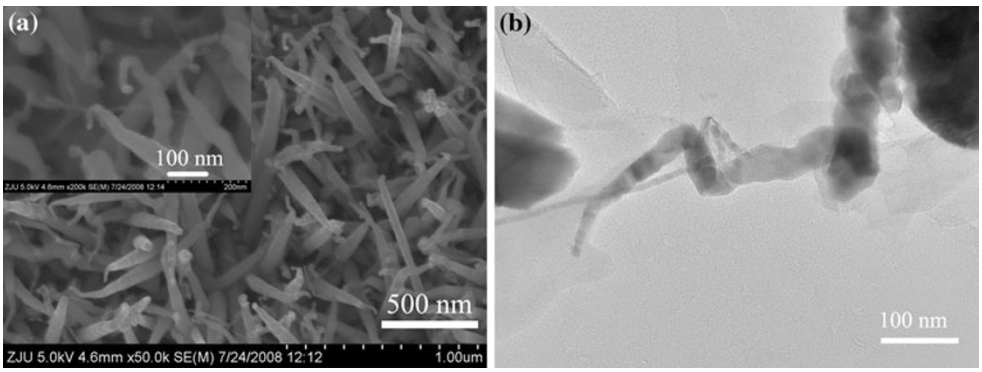

Fig. 4 **a** SEM (inset: higher magnification) and **b** TEM of In_2O_3 nanowires synthesized by annealing Cu–In compound for 0.5 h

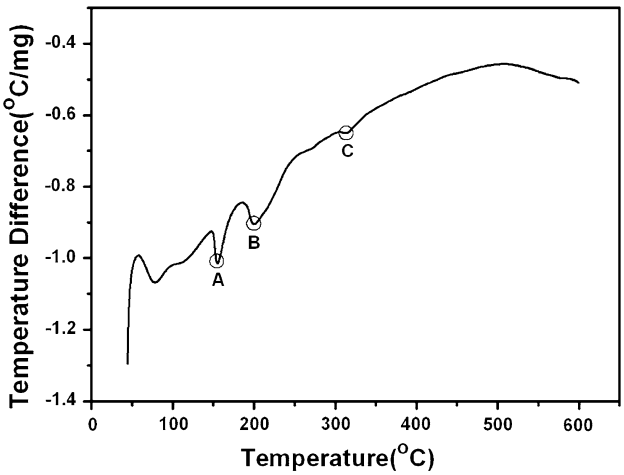

Fig. 5 Differential thermal analysis (DTA) of Cu–In compound in N_2 atmosphere

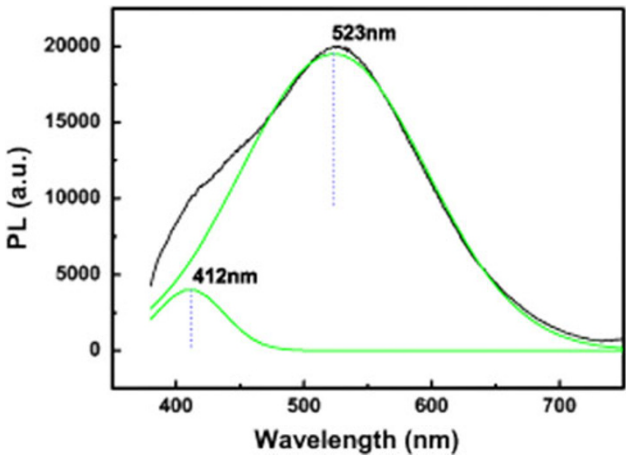

Fig. 6 PL from In_2O_3 nanowires measured at room temperature. The constituent PL peaks are indicated by *dashed lines*. The inset is the HRTEM image of a nanocrystalline InO particle

samples on glass and Cu substrates are shown in Fig. 3. The annealing condition is the same as that for Cu–In compound. It can be seen that nanowires are formed after annealing In particles on a Cu substrate (Fig. 3b), while the sphere shape of particles is kept after annealing one on a glass substrate (Fig. 3a. The XRD patterns of the corresponding products in Fig. 3c verify that In particles on glass are partly oxidized to In_2O_3 particles, whereas little hints of In is found from the products and Cu substrate. Moreover, the lattice spacing of 0.36 nm in the inset of Fig. 3b matches well with the (220) crystal plane of In_2O_3. This experiment verifies again that Cu plays an important catalyst rule on the formation of In_2O_3 nanowires. Without Cu, In cannot be transferred into In_2O_3 nanowires even if it is annealed at 550°C.

Since long nanowires are entangled, it is suspected that Cu particles as catalysts in this experiment are not as easily identified as Au particles [15–18]. In order to obtain shorter In_2O_3 nanowires, In–Cu compound was annealed for only 0.5 h. The SEM and TEM images of the compound are shown in Fig. 4. It can be seen that with a short annealing time the products are more like nanotowers, thicker at the beginning and thinner at the top. The "particle-like" contrasts on the top of nanowires in the inset of Fig. 4a are considered to be a zigzag characteristic of short nanowires. Moreover, the TEM image in Fig. 4b illustrates that no metal particles are obviously observed on the top of a nanotower as the previous report [17]. That means that the In_2O_3 nanostructures are formed via a different catalyst-assisted growth mechanism from VS or VLS mechanism.

The DTA data shown in Fig. 5 indicate the change of phase during the annealing of Cu–In compound. Point A is related to the melting of In particles; point B results from the transformation of CuIn to $Cu_{11}In_9$ and In; point C indicates the decomposition of $Cu_{11}In_9$, leading to the formation of thermal equilibrium compositions of $Cu_{16}In_9$ and In, as same as reported in [23]. It is clear that after annealing at lower temperatures, In elements will be driven out of Cu–In compound. At about 530°C a clear tendency of increase in weight is seen in Fig. 5. This means that In element is oxidized, as reported in [24], while oxygen may come from the leakage of CVD chamber or unpurified

gases (esp. N_2). In fact, it was reported before that In is easy to oxidize, which has been observed even under ultra-high vacuum in previous work [23, 25].

Zheng reported that In_2O_3 nanowires could be obtained by vaporizing In particles at a high temperature of 900°C via VS mechanism [14]. However, in this study, solid In and a lower annealing temperature were employed. Therefore, In_2O_3 nanowires should not be grown via VS mechanism. In fact, at such a low temperature of 550°C, solid In should not be vaporized. Moreover, according to the results of Figs. 1, 2, 3, it is clear to confirm that Cu plays a catalyst rule in the formation of the nanowires via a different mechanism.

On the basis of the above-mentioned results, it is suggested that In either in as-grown compound or driving out from Cu–In compound can work for the growth of In_2O_3. During annealing at $\sim$550°C, Cu–In compound transfers to the liquid form in an In–rich condition according to Cu–In phase diagram. Hence, Cu–In liquid droplets can be formed in the part of Cu–In compound in the initial stage of annealing. And then, the rest of Cu–In compound is possibly "passivated" by oxidation, and ultimately retains a solid phase. In this case, the first solid–liquid interface between solid and liquid Cu–In compound is formed. Later, supersaturated In in Cu–In compound will segregate from the liquid droplets to interact with oxygen and to form In_2O_3 solid. A second liquid–solid interface between liquid Cu–In compound and In_2O_3 solid is formed, resulting in the growth of In_2O_3 nanowires [26]. This growth mechanism is related to two liquid–solid interfaces and three different phases, so-called solid–liquid–solid (SLS) mechanism, which is analogous to vapor–liquid–solid (VLS) mechanism. Since the In source supply is diffusion-limited, the In_2O_3 nanostructure is thicker at the bottom and snagged thinner and thinner at the top as annealing time increases, as indicated in Figs. 1b and 4a.

We also measured the PL spectra of the In_2O_3 nanowires, as shown in Fig. 6. The peaks at around 412 and 523 nm are observed, which are not from quantum confinement effect since the dimensions of the nanowires in our experiments are beyond the range of the Bohr diameter of an exciton in In_2O_3 (between 2.6 and 5 nm) [27]. It is assumed that the blue emission peak with a small shoulder at 412 nm originates from the exciton combination [10]. The process of exciton formation is closely related to oxygen vacancies ($V_O^{\times}$) as demonstrated by electron paramagnetic resonance (EPR) [28]. The PL peak at around 520 nm is rarely observed in vacancy-related emission to our knowledge. Zhou et al. ascribed the PL peak at 520 nm to amorphous InO nanoparticles, the size of which was semiquantitatively determined to be 6 nm [29]. Therefore, the light emission around 520 nm may be also from amorphous InO nanoparticles in the amorphous phases around In_2O_3 nanowires, which are indicated in Fig. 1d. We believe that the reducing environment at a relatively low annealing temperature contributes to the formation of amorphous InO nanoparticles and oxygen vacancies.

Conclusion

In_2O_3 nanowires have been synthesized by simply annealing Cu–In compound particles at a relatively low temperature of 550°C. It is found that Cu catalyzes the growth of In_2O_3 nanowires, while In as the source may be segregated from the Cu–In compound. On the basis of the results, an SLS growth mechanism of In_2O_3 nanowires is suggested. Finally, the peaks in the PL spectra of In_2O_3 nanowires at 412 and 523 nm were considered to originate from oxygen vacancies and amorphous InO nanoparticles, respectively.

Acknowledgments The authors thank Jieru Wang and Guoliang Xu for their kind help for characterization, and Jipeng Cheng for his deep discussion in experiments. We acknowledge financial support from 973 Program (2007CB613403).

References

1. J.Y. Lao, J.Y. Huang, D.Z. Wang, Z.F. Ren, Adv. Mater. **16**, 65 (2004)
2. H.Q. Yang, R.G. Zhang, H.X. Dong, J. Yu, W.Y. Yang, D.H. Chen, Cryst. Growth Des. **8**, 3154 (2008)
3. P. Nguyen, H.T. Ng, T. Yamada, M.K. Smith, J. Li, J. Han, M. Meyyappan, Nano Lett. **4**, 651 (2004)
4. H.B. Jia, Y. Zhang, X.H. Chen, J. Shu, X.H. Luo, Z.S. Zhang, D.P. Yu, Appl. Phys. Lett. **82**, 4146 (2003)
5. D.H. Zhang, Z.Q. Liu, C. Li, T. Tang, X.L. Liu, S. Han, B. Lei, C.W. Zhou, Nano Lett. **4**, 1919 (2004)
6. C. Li, D.H. Zhang, X.L. Liu, S. Han, T. Tang, J. Han, C.W. Zhou, Appl. Phys. Lett. **82**, 1613 (2003)
7. M. Curreli, C. Li, Y.H. Sun, B. Lei, M.A. Gundersen, M.E. Thompson, C.W. Zhou, J. Am. Chem. Soc. **127**, 6922 (2005)
8. H.F. Yang, Q.H. Shi, B.Z. Tian, Q.Y. Lu, F. Gao, S.H. Xie, J. Fan, C.Z. Yu, B. Tu, D.Y. Zhao, J. Am. Chem. Soc. **125**, 4724 (2003)
9. M.J. Zheng, L.D. Zhang, G.H. Li, X.Y. Zhang, Appl. Phys. Lett. **79**, 839 (2001)
10. X.C. Wu, J.M. Hong, Z.J. Han, Y.R. Tao, Chem. Phys. Lett. **373**, 28 (2003)
11. P. Wu, Q. Li, C.X. Zhao, L.F. Chi, T. Xiao, Appl. Surf. Sci. **255**, 3201 (2008)
12. Z.Y. Huang, C.F. Chai, X.C. Tan, J. Wu, A.Q. Yuan, Z.G. Zhou, Mater. Lett. **61**, 5137 (2007)
13. D.A. Magdas, A. Cremades, J. Piqueras, Appl. Phys. Lett. **88**, 113107 (2006)

14. F.H. Zheng, X. Zhang, J. Wang, L.S. Wang, L.N. Zhang, Nanotechnology **15**, 596 (2004)
15. C.H. Liang, G.W. Meng, Y. Lei, F. Philipp, L.D. Zhang, Adv. Mater. **13**, 1330 (2001)
16. M.C. Johnson, S. Aloni, D.E. McCready, E.D. Bourret-Courchesne, Cryst. Growth Des. **6**, 1936 (2006)
17. S. Kar, S. Chaudhuri, Chem. Phys. Lett. **422**, 424–428 (2006)
18. C.J. Chen, W.L. Xu, M.Y. Chern, Adv. Mater. **19**, 3012 (2006)
19. J. Zhang, X. Qing, F.H. Jiang, Z.H. Dai, Chem. Phys. Lett. **371**, 311 (2003)
20. D. Calestani, M.Z. Zha, A. Zappettini, L. Lazzarini, L. Zantti, Chem. Phys. Lett. **445**, 251 (2007)
21. J. Arbiol, B. Kalache, P.R. Cabarrocas, J.R. Morante, A.F. Morral, Nanotechnology **18**, 305606 (2007)
22. K. Kang, D.A. Kim, H.S. Lee, C.J. Kim, J.E. Yang, M.H. Jo, Adv. Mater. **20**, 1 (2008)
23. M. Gossia, H. Metzner, H.E. Mahnke, J. Appl. Phys. **86**, 3624 (1999)
24. P.K. Khanna, K.W. Jun, K.B. Hong, J.O. Baeg, R.C. Chikate, B.K. Das, Mater. Lett. **59**, 1032 (2005)
25. M. Gossla, H.E. Mahnke, H. Metzner, Thin Solid Films **361**, 56 (2000)
26. H.F. Yan, Y.J. Xing, Q.L. Hang, D.P. Yu, Y.P. Wang, J. Xu, Z.H. Xi, S.Q. Feng, Chem. Phys. Lett. **323**, 224 (2000)
27. W.S. Seo, H.H. Jo, K. Lee, J.T. Park, Adv. Mater. **15**, 795 (2003)
28. P. Guha, S. Kar, S. Chaudhuri, Appl. Phys. Lett. **85**, 3851 (2004)
29. H.J. Zhou, W.P. Cai, L.D. Zhang, Appl. Phys. Lett. **75**, 495 (1999)